

# DYNAMIC TRANSITIONS AND BAROCLINIC INSTABILITY FOR 3D CONTINUOUSLY STRATIFIED BOUSSINESQ FLOWS

TAYLAN ŞENGÜL AND SHOUHONG WANG

**ABSTRACT.** The main objective of this article is to study the nonlinear stability and dynamic transitions of the basic (zonal) shear flows for the three-dimensional continuously stratified rotating Boussinesq model. The model equations are fundamental equations in geophysical fluid dynamics, and dynamics associated with their basic zonal shear flows play a crucial role in understanding many important geophysical fluid dynamical processes, such as the meridional overturning oceanic circulation and the geophysical baroclinic instability. In this paper, first we derive a threshold for the energy stability of the basic shear flow, and obtain a criteria for nonlinear stability in terms of the critical horizontal wavenumbers and the system parameters such as the Froude number, the Rossby number, the Prandtl number and the strength of the shear flow. Next we demonstrate that the system always undergoes a dynamic transition from the basic shear flow to either a spatiotemporal oscillatory pattern or circle of steady states, as the shear strength  $\Lambda$  of the basic flow crosses a critical threshold  $\Lambda_c$ . Also we show that the dynamic transition can be either continuous or catastrophic, and is dictated by the sign of a transition parameter  $A$ , fully characterizing the nonlinear interactions of different modes. Both the critical shear strength  $\Lambda_c$  and the transition number  $A$  are functions of the system parameters. A systematic numerical method is carried out to explore transition in different flow parameter regimes. In particular, our numerical investigations show the existence of a hypersurface  $\Lambda = \Lambda_c$  which separates the parameter space into regions where the basic shear flow is stable and unstable. Numerical investigations also yield that the selection of horizontal wave indices at fixed  $Fr$ ,  $Pr$ ,  $Ro$  is determined only by  $L_y$ , the  $y$ -length scale of the box. We find that the system admits only critical eigenmodes with horizontal wave indices  $(0, m_y)$ . Such modes, horizontally have the pattern consisting of  $m_y$ -rolls aligned with the  $x$ -axis. Furthermore, numerically we encountered continuous transitions to multiple steady states, continuous and catastrophic transitions to spatiotemporal oscillations.

## 1. INTRODUCTION AND MAIN RESULTS

The atmosphere and the oceans are extremely rich in their organization and complexity, and many phenomena that they exhibit, involving a broad range of temporal and spatial scales [4], cannot be reproduced in the laboratory. The behavior of the atmosphere, the ocean, or the coupled atmosphere and ocean can be viewed as an initial and boundary value problem [1, 20, 19]. According to [24], depending on the time scale of the phenomenon under consideration, or equivalently, on how far into the future one is attempting to make predictions of atmospheric conditions. It is convenient, then, to consider motions corresponding to short-, medium-, and long-term behavior of the atmosphere.

The ideas of dynamical systems theory were pioneered in [11, 12, 21, 22, 23, 9, 6, 7], among many others, whose authors explored the dynamics of low-order models of atmospheric and oceanic flows. The formulation of the primitive equations of atmosphere and ocean as an infinite-dimensional dissipative dynamical system were initiated in [10]. It is evident that geophysical fluid flows and climate variability exhibit recurrent large-scale patterns which are directly linked to dynamical

---

*Date:* May 9, 2017.

*Key words and phrases.* baroclinic instability, shear flow instability, continuously stratified Boussinesq flows, dynamic transition, center manifold reduction, continuous transition, catastrophic transition, random transition.

This research is supported in part by the National Science Foundation (NSF) grant DMS-1515024, and by the Office of Naval Research (ONR) grant N00014-15-1-2662.

processes represented in the governing dissipative dynamical system of the atmosphere and the ocean. The study of the persistence of these patterns and the transitions between them are of fundamental importance in geophysical fluid dynamics and climate dynamics.

The main objective of this paper is to study stability and dynamic transitions of a basic shear flow, associated with geophysical baroclinic instability, for the three dimensional (3D) continuously stratified rotating Boussinesq model. Baroclinic instability is one of the most important geophysical fluid dynamical instability, and plays a crucial role in understanding the dominant mechanism shaping the cyclones and anticyclones that dominate weather in mid-latitudes, as well as the mesoscale eddies that play various roles in oceanic dynamics and the transport of tracers.

The first analytic study of the problem was made by Eric Eady [8], Joseph Pedlosky [18] in the context of a single unstable baroclinic wave, followed by the work of Mak [17], Cai and Mak [3] and Cai [2], among many others. In view of all the previous work for this problem and to the best of our knowledge, the study of nonlinear stability and dynamic transitions of the basic shear flows, however, is still open.

Also, the previous studies on baroclinic instability are based on simplified models such as the 3D quasi-geostrophic model and multi-layer (in vertical) models. The model we adopt in this article is the 3D rotating continuously stratified Boussinesq equations, which are fundamental equations in geophysical fluid dynamics. They describe the conservation of mass, the conservation of momentum, coupled with the first law of thermodynamics, under the Boussinesq assumption that the density is constant except in the buoyancy term and in the equation of state.

The basic shear flow, in its nondimensional form, is given by (2.3):

$$\mathbf{u}_{ss} = (\Lambda z, 0, 0), \quad p_{ss} = -\frac{\Lambda}{\text{Ro}} yz, \quad \rho_{ss} = \frac{\text{Fr}^2 \Lambda}{\text{Ro}} y,$$

where  $\mathbf{u}_{ss}$  is the vertically dependent zonal shear velocity,  $p_{ss}$  and  $\rho_{ss}$  are the corresponding pressure and density fields. Here Fr is the Froude number,  $\Lambda$  is the (non-dimensional) strength of the basic shear flow, Pr is the Prandtl number and Ro is the Rossby number. For simplicity of the analysis and presentation, we use periodicity in the horizontal directions coupled with no-slip boundary conditions in the vertical direction for the deviation fields.

We now describe the main results of this paper.

First, we find a threshold for the energy stability of the system. We prove that if

$$\Lambda < \text{Fr}^4 \text{Ro} \text{Pr} \pi^4,$$

then for any initial data, the energy of the deviation field decays in the  $L^2$ -norm at least exponentially in time. This result suggests that increasing any of the parameters Fr, Ro, Pr has a stabilizing effect whereas increasing  $\Lambda$  has a destabilizing effect on the basic shear flow.

Next we turn our attention to the linear stability problem. Due to the periodicity of the system in the horizontal directions, the determination of the eigenpairs of the linear operator is reduced to the study of the eigenvalue problem corresponding to the z-direction of the eigenvectors. The resulting equations for non-zero horizontal wave numbers  $\alpha$  have to be solved numerically. We use a Legendre-Galerkin method to solve these equations which provides a very efficient method for the determination of the eigenpairs.

Studying the eigenvalue problem analytically, we show that if the wavenumber  $\alpha_c$  corresponding to the eigenvalue with largest real part satisfies

$$\alpha_c^2 > \left( \frac{1}{\text{Fr}^4} + \frac{\sqrt{2}}{\text{Ro}} \right) \max \left\{ \left( \frac{\Lambda^2}{\text{Pr}} \right)^{1/3}, \frac{1}{\text{Pr}} \right\}$$

then the system is nonlinearly stable.

Our numerical experiments with the linearized eigenvalue problem show the existence of a critical parameter  $\Lambda_c$  for which the eigenvalue  $\beta_c$  with the largest real part, the critical eigenvalue, crosses

the imaginary axis at  $\Lambda = \Lambda_c$ . Since we are not able to find an analytical expression for  $\Lambda_c$  in terms of other system parameters, we are led to numerical explorations of this critical parameter.

One of the main issues in this paper is the identification of the first transition which takes place at  $\Lambda = \Lambda_c$ . The first transition of the basic shear flow depends on the dimension of the critical eigenspace. Due to the periodicity condition in the horizontal directions, the first critical eigenspace spanned by the critical eigenmodes is always even dimensional, generically two. Thus we study the critical crossing of double real eigenvalues and a pair of complex conjugate eigenvalues separately.

The critical crossing of double real eigenvalues lead to a first transition of the basic shear flow to multiple steady states while the critical crossing of complex pair of eigenvalues lead to a first transition to a spatial-temporal oscillations (time periodic solutions). In both cases, as the shear strength  $\Lambda$  crosses the critical value  $\Lambda_c$ , the system undergoes a continuous transition or catastrophic transition from the basic shear flow, dictated by a common parameter  $A$ , which characterizes precisely the interactions between different modes of the system.

In the case of transition to multiple steady states, we show the existence of a circle of degenerate steady states bifurcating at  $\Lambda = \Lambda_c$ .

We also prove a new representation for the approximation of the center manifold function for the critical crossing of complex conjugate pair of eigenvalues which is suitable for studying problems which are extended periodically in at least one spatial direction. This representation leads to the determination of a transition number which describes the critical crossing of both double real eigenvalues and a pair of complex conjugate eigenvalues together.

We show that the type of transition is determined by a parameter  $A$  which characterizes the nonlinear interactions between critical modes with modes having zero wave number and modes having twice the critical wave number. In our numerical investigations we encounter both continuous and catastrophic transitions to spatiotemporal oscillations and continuous transitions to multiple steady states.

With regards to the pattern formation after the transition, our numerical experiments suggest that the system always prefers rolls parallel to the east-west direction regardless of the east west length scale ratio.

This paper arises out of a research program to generate rigorous mathematical results on geophysical fluid dynamics and on climate variability developed from the viewpoint of dynamical transitions. This type of physically-induced stability and transition leads naturally for us to search for the full set of transition states, represented by a local attractor, giving a complete characterization of stability and transition. Such study was initiated in early 2000 by Ma and Wang, and the corresponding dynamical transition theory and its various applications are synthesized in [16]; we have shown in particular that the transitions of all dissipative systems can be classified into three classes: continuous, catastrophic and random, which correspond to very different dynamical transition behavior of the system. We refer interested readers to [16, 14, 15] and the references therein for a wide range of applications of the theory, as well as the recent work [5, 25] for dynamic transition of shear flows.

The paper is organized as follows. Section 2 introduces the model and its mathematical setting. Section 3 proves a nonlinear energy stability of the basic shear flow, and Section 4 characterizes linear instability and the principle of exchange of stabilities (PES). A nonlinear stability theorem is proved in Section 5 under a condition on the horizontal critical wave numbers. The main dynamic transition theorem, Theorem 6.1, of the paper is stated in Section 6 and proved in Section 7. Sections 8 and 9 are devoted to numerical investigations of the dynamic transitions of the basic shear flow on various parameter regimes, and Section 10 provides a brief conclusion of the main results in this paper.

## 2. MODEL EQUATIONS

The dimensional equations describing the baroclinicity for continuously stratified Boussinesq flow is given by

$$(2.1) \quad \begin{aligned} \mathbf{u}_t + (\mathbf{u} \cdot \nabla) \mathbf{u} - \nu \Delta \mathbf{u} + \omega \hat{e}_3 \times \mathbf{u} + \frac{1}{\rho_0} \nabla p + \frac{1}{\rho_0} \rho g \hat{e}_3 &= 0, \\ \rho_t + (\mathbf{u} \cdot \nabla) \rho - \kappa \Delta \rho &= 0, \\ \nabla \cdot \mathbf{u} &= 0. \end{aligned}$$

Here  $\mathbf{u}$  is the velocity field,  $p$  is the pressure,  $\rho$  is the density (temperature),  $\nu$  is the kinematic viscosity,  $\omega$  is the planetary rotation rate,  $\hat{e}_e$  is the unit vector in the  $z$  direction,  $\rho_0$  is a reference density,  $g$  is the gravitation constant, and  $\kappa$  is the thermal diffusivity. It is assumed that the fluid resides in a container with dimensional height  $h$ .

We nondimensionalize the equations (2.1) using

$$x = hx', \quad t = \frac{h^2}{\kappa} t', \quad \mathbf{u} = \frac{\kappa}{h} \mathbf{u}', \quad \rho = \rho_0 \rho',$$

and drop primes to obtain

$$(2.2) \quad \begin{aligned} \mathbf{u}_t + (\mathbf{u} \cdot \nabla) \mathbf{u} - \text{Pr} \Delta \mathbf{u} + \frac{1}{\text{Ro}} \hat{e}_3 \times \mathbf{u} + \nabla p + \frac{1}{\text{Fr}^2} \rho \hat{e}_3 &= 0, \\ \rho_t + (\mathbf{u} \cdot \nabla) \rho - \Delta \rho &= 0, \\ \nabla \cdot \mathbf{u} &= 0, \end{aligned}$$

where the nondimensional numbers are defined as

$$\text{Pr} = \frac{\nu}{\kappa}, \quad \text{Ro} = \frac{[U]}{[L]\omega} = \frac{\kappa}{h^2\omega}, \quad \text{Fr}^2 = \frac{[U]^2}{[L]g} = \frac{\kappa^2}{gh^3}.$$

The equations (2.2) admit the following steady state solution characterizing a shearing motion which, due to the Coriolis forces, must be balanced by a pressure gradient in response to spatially varying density field:

$$(2.3) \quad \mathbf{u}_{ss} = (\Lambda z, 0, 0), \quad p_{ss} = -\frac{\Lambda}{\text{Ro}} yz, \quad \rho_{ss} = \frac{\text{Fr}^2 \Lambda}{\text{Ro}} y.$$

Taking the deviations from the basic state

$$\mathbf{u}' = \mathbf{u} - \mathbf{u}_{ss}, \quad p' = p - p_{ss}, \quad \rho' = \rho - \rho_{ss},$$

and dropping the primes, we deduce the following equations for the deviations:

$$(2.4) \quad \begin{aligned} \mathbf{u}_t + (\mathbf{u} \cdot \nabla) \mathbf{u} + \Lambda z \frac{\partial \mathbf{u}}{\partial x} + \Lambda \omega \hat{e}_3 - \text{Pr} \Delta \mathbf{u} + \frac{1}{\text{Ro}} \hat{e}_3 \times \mathbf{u} + \nabla p + \frac{1}{\text{Fr}^2} \rho \hat{e}_3 &= 0, \\ \rho_t + (\mathbf{u} \cdot \nabla) \rho + \frac{\Lambda}{\text{RoFr}^2} y - \Delta \rho &= 0, \\ \nabla \cdot \mathbf{u} &= 0, \end{aligned}$$

in the nondimensional rectangular domain  $(x, y, z) \in \Omega = (0, L_x) \times (0, L_y) \times (0, 1)$ .

In this study, we consider the periodic boundary conditions in the  $x$  and  $y$  directions with periods  $L_x$  and  $L_y$  for simplicity. In the  $z$  direction we consider no-slip boundary conditions:

$$(2.5) \quad u = v = w = \rho = 0, \quad \text{at } z = 0, 1.$$

We also want to give a remark for the case of free-slip boundary conditions, i.e. the Neumann boundary conditions for the horizontal velocities in the vertical direction. In the case of free-slip boundaries, the linear problem will always have a pair of eigenvalues with zero real part. Thus the principle of exchange of stability will be no longer valid and the reduction to the center manifold, necessary for the analysis of the transition, will not be justified.

The functional setting of the problem can be cast as follows. Let

$$X_1 = \{(\mathbf{u}, \rho) \in H^2(\Omega, \mathbb{R}^4) : \nabla \cdot \mathbf{u} = 0, \mathbf{u}|_{z=0,1} = 0, \rho|_{z=0,1} = 0\}$$

and

$$X = \{(\mathbf{u}, \rho) \in L^2(\Omega, \mathbb{R}^4) : \nabla \cdot \mathbf{u} = 0, \mathbf{u}|_{z=0,1} = 0, \rho|_{z=0,1} = 0\}$$

where the spaces denote the usual Sobolev spaces such that  $\mathbf{u}, \rho$  are periodic in  $x$  and  $y$  with periods  $L_x$  and  $L_y$ .

Now the main equations can be cast as

$$(2.6) \quad \frac{d\phi}{dt} = L\phi + G(\phi), \quad \phi = (\mathbf{u}, \rho),$$

where  $L : X_1 \rightarrow X$  is the linear operator and  $G : X_1 \times X_1 \rightarrow X$  is the nonlinear operator, defined by

$$(2.7) \quad \begin{aligned} L\phi &= -\mathcal{P} \begin{pmatrix} \Lambda z \frac{\partial \mathbf{u}}{\partial x} + \Lambda w \hat{e}_3 - \text{Pr} \Delta \mathbf{u} + \frac{1}{\text{Ro}} \hat{e}_3 \times \mathbf{u} + \frac{1}{\text{Fr}^2} \rho \hat{e}_3 \\ \frac{\Lambda}{\text{RoFr}^2} v - \Delta \rho \end{pmatrix}, \\ G(\phi, \tilde{\phi}) &= -\mathcal{P} \begin{pmatrix} (\mathbf{u} \cdot \nabla) \mathbf{u} \\ (\mathbf{u} \cdot \nabla) \rho \end{pmatrix}, \\ G(\phi) &= G(\phi, \phi). \end{aligned}$$

Here  $\mathcal{P} : L^2(\Omega, \mathbb{R}^4) \rightarrow X$  is the standard Leray projection.

### 3. ENERGY STABILITY

In this section, we address the energy stability of the basic shear flow. We will use  $\|\cdot\|$  to denote the  $L^2(\Omega)$  norm.

**Theorem 3.1.** *If*

$$(3.1) \quad \Lambda < \text{Fr}^4 \text{RoPr} \pi^4,$$

*then the energy*

$$(3.2) \quad E = \|\mathbf{u}\|^2 + \frac{\text{Ro}}{\Lambda} \|\rho\|^2$$

*decays in the  $L^2$  norm at least exponentially in time.*

*Proof.* Taking  $L^2$  inner product between the first two equations of (2.4) and  $(\mathbf{u}, \rho)$ , we obtain

$$(3.3) \quad \frac{d\|\mathbf{u}\|^2}{2dt} + \Lambda \|w\|^2 + \text{Pr} \|\nabla \mathbf{u}\|^2 + \frac{1}{\text{Fr}^2} \int_{\Omega} \rho w dV = 0,$$

$$(3.4) \quad \frac{d\|\rho\|^2}{2dt} + \frac{\Lambda}{\text{RoFr}^2} \int_{\Omega} v \rho dV + \|\nabla \rho\|^2 = 0.$$

We derive from (3.2), (3.3) and (3.4) that

$$\frac{dE}{2dt} = -\Lambda \|w\|^2 - \text{Pr} \|\nabla \mathbf{u}\|^2 - \frac{1}{\text{Fr}^2} \int_{\Omega} \rho(w + v) dV - \frac{\text{Ro}}{\Lambda} \|\nabla \rho\|^2.$$

Using the Poincare inequalities (thanks to the no-slip boundary conditions):

$$\|\nabla \mathbf{u}\|^2 \geq \pi^2 \|\mathbf{u}\|^2, \quad \|\nabla \rho\|^2 \geq \pi^2 \|\rho\|^2,$$

we obtain that

$$(3.5) \quad \frac{dE}{2dt} \leq -\Lambda \|w\|^2 - \text{Pr} \pi^2 \|\mathbf{u}\|^2 - \frac{1}{\text{Fr}^2} \int_{\Omega} \rho(w + v) dV - \frac{\text{Ro}\pi^2}{\Lambda} \|\rho\|^2.$$

By the Cauchy-Schwarz and the Young inequalities, we have

$$\left| \int_{\Omega} \rho(w+v) dV \right| \leq \epsilon \|\rho\|^2 + \frac{1}{2\epsilon} \|w\|^2 + \frac{1}{2\epsilon} \|v\|^2 \leq \epsilon \|\rho\|^2 + \frac{1}{2\epsilon} \|\mathbf{u}\|^2.$$

Consequently, dropping the  $-\Lambda\|w\|^2$  term, we infer from (3.5) that

$$\frac{dE}{2dt} \leq (-\text{Pr} \pi^2 + \frac{1}{2\text{Fr}^2\epsilon}) \|\mathbf{u}\|^2 + (-\frac{\text{Ro}\pi^2}{\Lambda} + \frac{\epsilon}{\text{Fr}^2}) \|\rho\|^2.$$

Choosing  $\epsilon = \frac{\text{Fr}^2\text{Ro}\pi^2}{2\Lambda}$ , we arrive at

$$\frac{dE}{2dt} \leq \left( -\text{Pr} \pi^2 + \frac{\Lambda}{\text{Fr}^4\text{Ro}\pi^2} \right) \|\mathbf{u}\|^2 - \frac{\text{Ro}\pi^2}{2\Lambda} \|\rho\|^2.$$

By (3.1),  $\text{Pr} \pi^2 - \frac{\Lambda}{\text{Fr}^4\text{Ro}\pi^2} > 0$ . Letting

$$c_0 = 2 \min \left\{ \text{Pr} \pi^2 - \frac{\Lambda}{\text{Fr}^4\text{Ro}\pi^2}, \frac{\pi^2}{2} \right\},$$

we finally obtain that

$$\frac{dE}{dt} \leq -c_0 E(t),$$

and the theorem follows.  $\square$

#### 4. SPECTRUM OF LINEARIZED PROBLEM AND PRINCIPLE OF EXCHANGE OF STABILITIES

**4.1. Linearized eigenvalue problem.** In this section we consider the eigenvalue problem associated with the linear part of the main equations (2.4):

$$\begin{aligned} (4.1) \quad & \text{Pr} \Delta \mathbf{u} - \Lambda z \frac{\partial \mathbf{u}}{\partial x} - \Lambda w \hat{e}_3 - \frac{1}{\text{Ro}} \hat{e}_3 \times \mathbf{u} - \nabla p - \frac{1}{\text{Fr}^2} \rho \hat{e}_3 = \beta \mathbf{u}, \\ & -\frac{\Lambda}{\text{RoFr}^2} v + \Delta \rho = \beta \rho, \\ & \nabla \cdot \mathbf{u} = 0, \end{aligned}$$

together with the boundary conditions (2.5).

The above eigenvalue system (4.1) and the boundary condition (2.5) can be solved using the ansatz

$$(4.2) \quad \phi_{m_x, m_y, m_z} = \begin{bmatrix} \mathbf{u} \\ \rho \end{bmatrix} = e^{i\left(\frac{m_x \pi x}{L_x} + \frac{m_y \pi y}{L_y}\right)} \begin{bmatrix} U_{m_x, m_y, m_z}(z) \\ V_{m_x, m_y, m_z}(z) \\ W_{m_x, m_y, m_z}(z) \\ R_{m_x, m_y, m_z}(z) \end{bmatrix},$$

where the horizontal wave vector and wave number are defined by:

$$(4.3) \quad \alpha = (\alpha_x, \alpha_y) = \left( \frac{m_x \pi}{L_x}, \frac{m_y \pi}{L_y} \right), \quad \alpha^2 = \alpha_x^2 + \alpha_y^2.$$

*Case  $\alpha = 0$ :* In this case, the corresponding eigenfunctions do not depend on  $x$  and  $y$ . In this case,  $\nabla \cdot \mathbf{u} = 0$  implies  $\frac{\partial w}{\partial z} = 0$ , hence  $w = 0$  due to the boundary conditions. Thus system (4.1)

reduces to

$$\begin{aligned} \Pr D^2 U + \frac{1}{\text{Ro}} V &= \beta U, \\ \Pr D^2 V - \frac{1}{\text{Ro}} U &= \beta V, \\ D^2 R - \frac{\Lambda}{\text{RoFr}^2} V &= \beta R, \\ U = V = R &= 0 \quad \text{at } z = 0, 1. \end{aligned}$$

The solutions can easily be found for  $m_z \in \mathbb{Z}^+$ , and are given by

$$(4.4) \quad \begin{aligned} \beta_{0,0,m_z}^1 &= -m_z^2 \pi^2, & \phi_{0,0,m_z}^1 &= [0, 0, 0, \sqrt{2} \sin m_z \pi z], \\ \beta_{0,0,m_z}^2 &= -\Pr m_z^2 \pi^2 - \frac{1}{\text{Ro}} i, & \phi_{0,0,m_z}^2 &= \left[ 1, i, 0, \frac{-i\Lambda/\text{Fr}^2}{i + m_z^2 \pi^2 (\Pr - 1) \text{Ro}} \right] \sin m_z \pi z, \\ \beta_{0,0,m_z}^3 &= \overline{\beta_{0,0,m_z}^2}, & \phi_{0,0,m_z}^3 &= \overline{\phi_{0,0,m_z}^2}. \end{aligned}$$

*Case  $\alpha \neq 0$ :* In this case (4.1) reduces to

$$(4.5) \quad \Pr(D^2 - \alpha^2)C - \Lambda i \alpha_x z C - \frac{1}{\text{Ro}} DW = \beta C,$$

$$(4.6) \quad \frac{1}{\text{Ro}} DC + \Pr(D^2 - \alpha^2)^2 W - \Lambda \alpha^2 W - \Lambda i \alpha_x (D(zDW) - \alpha^2 z W) + \frac{\alpha^2}{\text{Fr}^2} R = \beta(D^2 - \alpha^2)W,$$

$$(4.7) \quad -\frac{\Lambda}{\text{RoFr}^2 \alpha^2} (i \alpha_x C + i \alpha_y DW) + (D^2 - \alpha^2)R = \beta R,$$

$$(4.8) \quad C = W = DW = R = 0 \quad \text{at } z = 0, 1.$$

Here  $C$  is the vertical component of the vorticity,

$$(4.9) \quad \begin{aligned} -i \alpha_x V + i \alpha_y U &= C, \\ i \alpha_x U + i \alpha_y V &= -DW. \end{aligned}$$

The second condition in (4.9) is just a consequence of incompressibility. This condition also imposes the boundary condition  $DW = 0$  at  $z = 0, 1$  in (4.8). Note that the equations (4.9) can be solved to recover  $U$  and  $V$  from  $C$  and  $DW$ .

**4.2. Adjoint linear equations.** To describe the transition number we will also need the eigenvectors of the adjoint linear eigenvalue problem, given by

$$(4.10) \quad \begin{aligned} \Pr \Delta \mathbf{u}^* + \Lambda z \frac{\partial \mathbf{u}^*}{\partial x} - \Lambda w^* \hat{e}_3 + \frac{1}{\text{Ro}} \hat{e}_3 \times \mathbf{u}^* - \nabla p^* - \frac{\Lambda}{\text{RoFr}^2} \rho^* \hat{e}_2 &= \bar{\beta} \mathbf{u}^*, \\ -\frac{1}{\text{Fr}^2} w^* + \Delta \rho^* &= \bar{\beta} \rho^*, \\ \nabla \cdot \mathbf{u}^* &= 0. \end{aligned}$$

This eigenvalue problem can be solved with the same ansatz (4.2). The equations in the  $\alpha = 0$  case are

$$\begin{aligned} \Pr D^2 U - \frac{1}{\text{Ro}} V &= \beta U, \\ \Pr D^2 V + \frac{1}{\text{Ro}} U - \frac{\Lambda}{\text{RoFr}^2} R &= \beta V, \\ D^2 R &= \beta R. \end{aligned}$$

The corresponding eigenvalues for  $\beta_{0,0,m_z}^{k*} = \overline{\beta_{0,0,m_z}^k}$ ,  $k = 1, 2, 3$  and eigenvectors are:

$$(4.11) \quad \begin{aligned} \phi_{0,0,m_z}^{1*} &= [\Lambda, m_z^2 \pi^2 (1 - \text{Pr}) \text{Ro} \Lambda, 0, \text{Fr}^2 (1 + m^4 \pi^4 (1 - \text{Pr})^2 \text{Ro}^2)] \sin m_z \pi z, \\ \phi_{0,0,m_z}^{2*} &= [1, -i, 0, 0] \sin m_z \pi z, \\ \phi_{0,0,m_z}^{3*} &= \overline{\phi_{0,0,m_z}^2}. \end{aligned}$$

For  $\alpha \neq 0$ , the equations reduce to

$$(4.12) \quad \begin{aligned} \text{Pr}(D^2 - \alpha^2)C^* + \Lambda i \alpha_x z C^* + \frac{1}{\text{Ro}} DW^* + \frac{\Lambda}{\text{RoFr}^2} i \alpha_x R^* &= \overline{\beta} C^*, \\ -\frac{1}{\text{Ro}} DC^* + \text{Pr}(D^2 - \alpha^2)W^* - \Lambda \alpha^2 W^* + \Lambda i \alpha_x (D(zDW^*) - \alpha^2 z W^*) \\ &+ \frac{\Lambda i \alpha_y}{\text{RoFr}^2} DR^* = \overline{\beta} (D^2 - \alpha^2)W^*, \\ -\frac{1}{\text{Fr}^2} W^* + (D^2 - \alpha^2)R^* &= \overline{\beta} R^*, \\ C^* = W^* = DW^* = R^* &= 0 \quad \text{at } z = 0, 1. \end{aligned}$$

**4.3. Principle of exchange of stabilities (PES).** For each horizontal wave vector  $\alpha$ , the eigenvalues are ordered so that

$$\text{Re } \beta_{m_x, m_y, 1}(\lambda) \geq \text{Re } \beta_{m_x, m_y, 2}(\lambda) \geq \dots, \quad \text{for each } (m_x, m_y) \in \mathbb{Z} \times \mathbb{Z},$$

where  $\lambda = (\text{Fr}, \Lambda, \text{Ro}, \text{Pr})$ .

By (4.4), the eigenvalues have always negative real part when  $m_x = m_y = 0$ . Due to the horizontal periodicity of the problem, generically, an eigenvalue with nonzero horizontal wave number is either real with multiplicity two or is simple, non-real and its complex conjugate is also an eigenvalue.

Let

$$(4.13) \quad \alpha_c = (\alpha_x^c, \alpha_y^c) = \left( \frac{m_x^c \pi}{L_x}, \frac{m_y^c \pi}{L_y} \right), \quad \alpha_c = \sqrt{(\alpha_x^c)^2 + (\alpha_y^c)^2}$$

be the critical horizontal wave vector and critical horizontal wave number so that  $\text{Re } \beta_{m_x^c, m_y^c, 1}(\lambda)$  is the largest among all  $\text{Re } \beta_{m_x^c, m_y^c, m_z}(\lambda)$ .

For our transition theorem, we will assume the existence of a critical parameter

$$\Lambda_c = \Lambda_c(L_x, L_y, \text{Fr}, \text{Pr}, \text{Ro})$$

and integers  $(m_x^c, m_y^c) \in \mathbb{Z} \times \mathbb{Z} \setminus \{(0, 0)\}$  such that the following PES condition is satisfied:

$$(4.14) \quad \begin{aligned} \text{Re } \beta_{m_x^c, m_y^c, 1} &= \text{Re } \beta_{m_x^c, m_y^c, 2} \begin{cases} < 0 & \text{if } \Lambda < \Lambda_c, \\ = 0 & \text{if } \Lambda = \Lambda_c, \\ > 0 & \text{if } \Lambda > \Lambda_c, \end{cases} \\ \text{Re } \beta_{m_x, m_y, m_z}(\Lambda_c) &< 0 \quad \text{for } (m_x, m_y) \neq (m_x^c, m_y^c) \text{ or } m_z \notin \{1, 2\}. \end{aligned}$$

Note that the condition (5.1) assures that the eigenvalues lie on the left complex half plane if  $\Lambda$  is small enough. In the last section, we will show the existence of parameter regimes where the PES (4.14) is satisfied numerically.

By a general dynamic transition theorem [16, Theorem 2.1.5], as  $\Lambda$  crosses  $\Lambda_c$ , the system always undergoes a dynamic transition from the basic shear flow to one of the three types (continuous, catastrophic or random). The types and structure of the dynamic transition are then dictated by the nonlinear interactions of different modes, and the remaining part of the paper is devoted to detailed characterization of the dynamic transition.



## 5. NONLINEAR STABILITY

The following theorem gives a sufficient condition on the nonlinear stability of the basic solution, in terms of the system parameters and the wave number of the critical mode. The condition is not optimal and may further be enhanced.

We will denote the eigenvalue with the largest real part as the critical eigenvalue, the corresponding eigenvectors as the critical eigenvectors and corresponding wave number as the critical wavenumber.

**Theorem 5.1.** *Let  $\alpha_c = (\alpha_x^c, \alpha_y^c) = (\frac{m_x^c \pi}{L_x}, \frac{m_y^c \pi}{L_y})$  be the critical wave number as given in (4.13). If*

$$(5.1) \quad \alpha_c^2 > \left( \frac{1}{\text{Fr}^4} + \frac{\sqrt{2}}{\text{Ro}} \right) \max \left\{ \left( \frac{\Lambda^2}{\text{Pr}} \right)^{1/3}, \frac{1}{\text{Pr}} \right\},$$

*then the system is nonlinearly stable.*

*Proof.* We need to show that the real part of the critical eigenvalue is negative. Consider the critical eigenvalue and eigenvector of the problem (4.5)–(4.8).

Here we also use  $\|\cdot\|$  for the  $L^2(0, 1)$  norm. Then taking  $L^2$  inner product between (4.5)–(4.7) and  $(C, W, R)$ , we obtain that

$$(5.2) \quad -\mathcal{E}_1 - \Lambda i \alpha_x^c \mathcal{E}_2 + \mathcal{I} = \beta \mathcal{E}_3,$$

where

$$\begin{aligned} \mathcal{E}_1 &= \text{Pr}(\|DC\|^2 + \alpha_c^2 \|C\|^2) + \text{Pr}(\|D^2W\|^2 + 2\alpha_c^2 \|DW\|^2 + \alpha_c^4 \|W\|^4) \\ &\quad + \Lambda \alpha_c^2 \|W\|^2 + \|DR\|^2 + \alpha_c^2 \|R\|^2, \\ \mathcal{E}_2 &= \|z^{1/2}C\|^2 + \|z^{1/2}DW\|^2 + \alpha_c^2 \|z^{1/2}W\|^2, \\ \mathcal{E}_3 &= \|C\|^2 + \|DW\|^2 + \alpha_c^2 \|W\|^2 + \|R\|^2, \\ \mathcal{I} &= \int_0^1 \left( -\frac{1}{\text{Ro}} DW \overline{C} - \frac{1}{\text{Ro}} DC \overline{W} - \frac{\alpha_c^2}{\text{Fr}^2} R \overline{W} - iA\alpha_x^c C \overline{R} + i\mu\alpha_y^c DW \overline{R} \right) dz, \\ \mu &= \frac{\Lambda}{\text{RoFr}^2\alpha_c^2}. \end{aligned}$$

The real part of (5.2) implies that

$$\text{Re } \beta = \frac{-\mathcal{E}_1 + \text{Re } \mathcal{I}}{\mathcal{E}_3}.$$

The proof will be done if we can show that  $|\mathcal{I}| < \mathcal{E}_1$ .

We estimate  $|\mathcal{I}|$  as

$$(5.3) \quad |\mathcal{I}| \leq \text{Pr} \|DC\|^2 + \|DR\|^2 + \alpha_c^2 \|R\|^2 + \frac{\mu^2}{2} \|C\|^2 + \left( \frac{1}{\text{Ro}^2 \text{Pr}} + \frac{\alpha_c^2}{2\text{Fr}^4} + \frac{\mu^2 \alpha_c^2}{4} \right) \|W\|^2.$$

In view of (5.2) with (5.3), the condition  $|\mathcal{I}| < \mathcal{E}_1$  will be satisfied if

$$(5.4) \quad \frac{1}{\text{Ro}^2 \text{Pr}} + \frac{\alpha_c^2}{2\text{Fr}^4} + \frac{\mu^2 \alpha_c^2}{4} \leq \text{Pr} \alpha_c^4 \quad \text{and} \quad \frac{\mu^2}{2} \leq \text{Pr} \alpha_c^2.$$

Now we use the Young's inequality with  $p = 3/2$  and  $q = 3$  in the second inequality below

$$\left( \frac{1}{\text{Fr}^4} + \frac{\sqrt{2}}{\text{Ro}} \right)^3 \geq \left( \frac{1}{3\text{Fr}^4} + \frac{2}{3\text{Ro}} \right)^3 \geq \frac{1}{\text{Ro}^2 \text{Fr}^4}.$$

By (5.1) and the above estimate, we deduce that

$$\frac{\mu^2}{2} = \frac{\Lambda^2 \alpha_c^2}{2\text{Ro}^2 \text{Fr}^4 \alpha_c^6} \leq \frac{\Lambda^2 \alpha_c^2}{2\text{Ro}^2 \text{Fr}^4} \left( \frac{1}{\text{Fr}^4} + \frac{\sqrt{2}}{\text{Ro}} \right)^{-3} \frac{\text{Pr}}{\Lambda^2} \leq \text{Pr} \alpha_c^2$$

and, consequently, the second condition in (5.4) is satisfied.

Using the second condition in (5.4), the first condition in (5.4) will be satisfied if

$$(5.5) \quad \text{Pr} \alpha_c^4 - \frac{\alpha_c^2}{\text{Fr}^4} - \frac{2}{\text{Ro}^2 \text{Pr}} \geq 0.$$

By (5.1), and using  $(a+b)^2 \geq a^2 + b^2$  for positive  $a, b$ , we have

$$\text{Pr} \alpha_c^2 \geq \frac{1}{\text{Fr}^4} + \frac{\sqrt{2}}{\text{Ro}} \geq \frac{1}{2\text{Fr}^4} + \frac{1}{2} \sqrt{\frac{1}{\text{Fr}^8} + \frac{8}{\text{Ro}^2}},$$

which implies that (5.5) indeed holds. The proof is complete.  $\square$

**Remark.** A sufficient condition for the nonlinear stability of the system can also be stated in terms of the minimum wave number given by

$$\alpha_{\min} = \min \left\{ \sqrt{\left( \frac{m_x \pi}{L_x} \right)^2 + \left( \frac{m_y \pi}{L_y} \right)^2} : (m_x, m_y) \in \mathbb{Z} \times \mathbb{Z}, m_x^2 + m_y^2 \neq 0 \right\} = \min \left\{ \frac{\pi}{L_x}, \frac{\pi}{L_y} \right\}.$$

Noticing that  $\alpha_{\min} \leq \alpha_c$ , it follows that if  $\alpha_{\min}$  satisfies (5.1) then the system is nonlinearly stable.

## 6. MAIN DYNAMIC TRANSITION THEOREM

As mentioned earlier, by a general dynamic transition theorem [16, Theorem 2.1.5], as  $\Lambda$  crosses  $\Lambda_c$ , the system always undergoes a dynamic transition from the basic shear flow to one of the three types (continuous, catastrophic or random). In this section, we shall demonstrate that the types and structure of the dynamic transitions are dictated by the sign of the transition number to be defined below, which captures the nonlinear interactions of different modes. To this end, from now on we use the following notations for the eigenvalues and eigenvectors.

$$\begin{aligned} \phi_c &= \phi_{m_x^c, m_y^c, 1}, & \phi_{0, m_z} &= \phi_{0, 0, m_z}, & \phi_{2c, m_z} &= \phi_{2m_x^c, 2m_y^c, m_z}, \\ \phi_c^* &= \phi_{m_x^c, m_y^c, 1}^*, & \phi_{0, m_z}^* &= \phi_{0, 0, m_z}^*, & \phi_{2c, m_z}^* &= \phi_{2m_x^c, 2m_y^c, m_z}^*, \\ \beta_c &= \beta_{m_x^c, m_y^c, 1}, & \beta_{0, m_z} &= \beta_{0, 0, m_z}, & \beta_{2c, m_z} &= \beta_{2m_x^c, 2m_y^c, m_z}. \end{aligned}$$

We then define the transition number by

$$(6.1) \quad A = \sum_{m_z=1}^{\infty} A_{0, m_z} + A_{2, m_z},$$

where

$$\begin{aligned} A_{0, m_z} &= \frac{1}{\langle \phi_c, \phi_c^* \rangle} \Phi_{0, m_z} \langle G_s(\phi_c, \phi_{0, m_z}), \phi_c^* \rangle, \\ A_{2, m_z} &= \frac{1}{\langle \phi_c, \phi_c^* \rangle} \Phi_{2c, m_z} \langle G_s(\overline{\phi_c}, \phi_{2c, m_z}), \phi_c^* \rangle, \\ \Phi_{0, m_z} &= \frac{1}{-\beta_{0, m_z} \langle \phi_{0, m_z}, \phi_{0, m_z}^* \rangle} \langle G_s(\phi_c, \overline{\phi_c}), \phi_{0, m_z}^* \rangle, \\ \Phi_{2c, m_z} &= \frac{1}{(2i \text{Im}(\beta_c) - \beta_{2c, m_z}) \langle \phi_{2c, m_z}, \phi_{2c, m_z}^* \rangle} \langle G(\phi_c, \phi_c), \phi_{2c, m_z}^* \rangle. \end{aligned} \quad (6.2)$$

Here  $G_s(\phi_1, \phi_2) = G(\phi_1, \phi_2) + G(\phi_2, \phi_1)$  and  $G((\mathbf{u}_1, \rho_1), (\mathbf{u}_2, \rho_2)) = -\mathcal{P}(\mathbf{u}_1 \cdot \nabla(\mathbf{u}_2, \rho_2))$ ; see (2.7).

The numbers  $A_{0,j}$  and  $A_{2,j}$  represent the nonlinear interactions of the critical modes with the modes having wave numbers 0 and  $2\alpha_c$  respectively.

We note that the transition number  $A$  defined by (6.1) is valid for the critical crossing of both the complex and real eigenvalues, with the only difference being that  $\text{Im}(\beta_c) = 0$  in the last expression in (6.2) in the critical crossing of real eigenvalues.

The main dynamic transition theorem of the paper is as follows:

**Theorem 6.1.** *Assume that the PES condition (4.14) is valid.*

(1) *If  $\text{Im}(\beta_c) = 0$  near  $\Lambda = \Lambda_c$ , then the transition number  $A$  defined by (6.1) is real and the following statements hold true:*

(a) *If  $A < 0$ , then the original system (2.4) with (2.5) undergoes a continuous dynamic transition on  $\Lambda > \Lambda_c$  and bifurcates, on  $\Lambda > \Lambda_c$ , from the basic shear flow to an attracting circle of steady states:*

$$\Sigma_\Lambda = \left\{ 2\sqrt{\frac{-\beta_c}{A}} \text{Re}(e^{i\gamma}\phi_c) + O(|\beta_c|) : \gamma \in \mathbb{R} \right\}.$$

(b) *If  $A > 0$ , then the system (2.4) with (2.5) undergoes jump transition, and bifurcates, on  $\Lambda < \Lambda_c$ , from the basic shear flow to a repeller  $\Sigma_\Lambda$  having the same form as given above.*

(2) *If  $\text{Im}(\beta_c) \neq 0$  near  $\Lambda = \Lambda_c$ , then the transition number  $A$  is non-real and the following statements hold true:*

(a) *If  $\text{Re}(A) < 0$ , then the system undergoes a continuous transition, and bifurcates, on  $\Lambda > \Lambda_c$ , from the basic shear flow to a stable limit cycle given by*

$$(6.3) \quad \phi_{bif} = z(t)\phi_c + \overline{z(t)\phi_c},$$

where

$$(6.4) \quad z(t) = \sqrt{\frac{-\text{Re}(\beta_c)}{\text{Re}(A)}} \exp(i \text{Im}(\beta_c)t) + O(-\text{Re}(\beta_c)).$$

(b) *If  $\text{Re}(A) > 0$ , then the system undergoes a jump transition, and bifurcates, on  $\Lambda < \Lambda_c$ , from the basic shear flow to an unstable periodic solution having the same form as (6.3) and (6.4).*

## 7. PROOF OF THEOREM 6.1.

By the dynamic transition theory [16], the dynamical transition is fully captured by the reduced system of the original system to the center manifold associated with the unstable modes. Hence the central gravity of the proof is to derive the reduced system. For this purpose, we derive in Appendix A an approximation formula for the central manifold function adapted to the specific structure of the underlying system, and use it to prove the main theorem in this section.

Let  $E_1, E_2$  be as defined in Appendix A, and let

$$(7.1) \quad \Psi = z(t)\phi_c + \overline{z(t)\phi_c} \in E_1.$$

Using (A.5), we can show that the center manifold has the approximation

$$(7.2) \quad \Phi = \sum_{j=1}^{\infty} z^2 \Phi_{2c,j} \phi_{2c,j} + |z|^2 \Phi_{0,j} \phi_{0,j} + \overline{z^2 \Phi_{2c,j} \phi_{2c,j}} + o(2),$$

where the coefficients are as defined in (6.2). Letting  $\phi = \Psi + \Phi$  which amounts to considering the dynamics on the center manifold, taking projection onto the center-unstable space and using

$\langle \overline{\phi_c}, \phi_c^* \rangle = 0$ , we get

$$(7.3) \quad \frac{dz}{dt} = \beta_c z + \frac{1}{\langle \phi_c, \phi_c^* \rangle} \langle G(\Psi + \Phi), \phi_c^* \rangle.$$

The nonlinear term in (7.3) can be written as

$$\langle G(\Psi + \Phi), \phi_c^* \rangle = \sum_{j=1}^{\infty} \langle G_s(z\phi_c, \Phi_{0,j}\phi_{0,j}|z|^2), \phi_c^* \rangle + \langle G_s(\overline{z\phi_c}, \Phi_{2c,j}\phi_{2c,j}z^2), \phi_c^* \rangle + o(3).$$

Then the equation (7.3) becomes

$$(7.4) \quad \frac{dz}{dt} = \beta_c z + A|z|^2 z + o(3),$$

where  $A$  is defined by (6.1). In polar coordinates  $z(t) = |z|e^{i\gamma}$ , (7.4) is equivalent to

$$(7.5) \quad \begin{aligned} \frac{d|z|}{dt} &= \operatorname{Re}(\beta_c)|z| + \operatorname{Re}(A)|z|^3 + o(|z|^3), \\ \frac{d\gamma}{dt} &= \operatorname{Im}(\beta_c) + \operatorname{Im}(A)|z|^2 + o(|z|^3). \end{aligned}$$

To finalize the proof, thanks to the dynamical transition theorems [16], there remains to analyze the stability of the zero solution of (7.5).

In the case where  $\operatorname{Im} \beta_c = 0$ , if one carries out this reduction procedure using real eigenvectors  $e_1 = \operatorname{Re} \phi_c$ ,  $e_2 = \operatorname{Im} \phi_c$  then it is easily seen that the coefficient  $A$  must be real. Supposing  $\beta_c > 0$  and  $A < 0$ , it is easy to see from (7.4) that  $|z(t)| \rightarrow -\sqrt{\frac{-\beta_c}{A}}$  as  $t \rightarrow \infty$  and the solutions of (7.4) will evolve to a circle of steady state solutions.

In the case  $\operatorname{Im} \beta_c \neq 0$ ,  $A$  is non-real. For  $\operatorname{Re}(A) < 0$ , a periodic solution of (7.5) will bifurcate on  $\operatorname{Re} \beta_c > 0$  given by (6.4). If  $\operatorname{Re}(A) > 0$  then the system will evolve to an attractor far away from  $z = 0$  on  $\operatorname{Re} \beta_c > 0$ .

## 8. NUMERICAL STRATEGY

**8.1. Numerical Solution of the Eigenvalue Problem.** To solve (4.5)–(4.8), we use the spectral Legendre Galerkin method. For this, we first make the change of variable  $\tilde{z} = 2z - 1$ , which transforms the  $z$ -domain from  $[0, 1]$  to  $[-1, 1]$  and the derivative  $D = \frac{d}{dz} = 2\frac{d}{d\tilde{z}} = 2\tilde{D}$ . Next, we discretize the problem using the expansions

$$(8.1) \quad C = \sum_{i=0}^{N-1} \widehat{C}_i e_i^C(\tilde{z}), \quad W = \sum_{i=0}^{N-1} \widehat{W}_i e_i^W(\tilde{z}), \quad R = \sum_{i=0}^{N-1} \widehat{R}_i e_i^R(\tilde{z}).$$

The basis functions are the generalized Jacobi polynomials (compact combinations of Legendre polynomials) given by

$$\begin{aligned} e_i^C(\tilde{z}) &= e_i^R(\tilde{z}) = L_i(\tilde{z}) - \frac{i(1+i)}{(2+i)(3+i)} L_{i+2}(\tilde{z}), \\ e_i^W(\tilde{z}) &= L_i(\tilde{z}) + a_i L_{i+2}(\tilde{z}) + b_i L_{i+4}(\tilde{z}), \\ a_i &= -\frac{2(5+2i)(9+5i+i^2)}{(3+i)(4+i)(7+2i)}, \quad b_i = -1 - a_i. \end{aligned}$$

The basis functions satisfy the boundary conditions

$$e_i^C(\tilde{z}) = e_i^W(\tilde{z}) = D^2 e_i^W(\tilde{z}) = e_i^R(\tilde{z}) = 0, \quad \tilde{z} = -1, 1.$$

The discretization of the linear eigenvalue problem is done by plugging the expansions (8.1) in (4.5)–(4.8) and taking the inner products with basis functions. Then the resulting finite dimensional matrix eigenvalue problem is solved.

**8.2. The Numerical Computation of the Transition Number.** We now give a more detailed form of the transition number  $A$  given by (6.1) and described by the equations (6.2). We represent each eigenvector as

$$\phi = e^{i\alpha \cdot x} \psi, \quad \psi = [u, v, w, r]^T,$$

and we use

$$i\alpha_x u_c + i\alpha_y v_c + Dw_c = 0, \quad 2i\alpha_x u_{2c} + 2i\alpha_y v_{2c} + Dw_{2c} = 0.$$

Then the expressions in (6.2) can be written as

$$(8.2) \quad \begin{aligned} G(\phi_c, \phi_{0,m_z}) &= e^{i\alpha \cdot x} (u_c \partial_x + v_c \partial_y + w_c D) \phi_{0,m_z} = e^{i\alpha \cdot x} w_c D \psi_{0,m_z}, \\ G(\phi_{0,m_z}, \phi_c) &= (u_{0,m_z} \partial_x + v_{0,m_z} \partial_y) \phi_c = e^{i\alpha \cdot x} (i\alpha_x u_{0,m_z} + i\alpha_y v_{0,m_z} \partial_y) \psi_c, \\ G(\overline{\phi_c}, \phi_{2c}) &= e^{i\alpha \cdot x} (2D\overline{w_c} + \overline{w_c} D) \psi_{2c}, \quad G(\phi_{2c}, \overline{\phi_c}) = e^{i\alpha \cdot x} \left( \frac{1}{2} Dw_{2c} + w_{2c} D \right) \overline{\psi_c}, \\ G(\phi_c, \overline{\phi_c}) &= (Dw_c + w_c D) \overline{\psi_c}, \quad G(\phi_c, \phi_c) = e^{2i\alpha \cdot x} (-Dw_c + w_c D) \psi_c. \end{aligned}$$

Hence the transition number becomes

$$(8.3) \quad \begin{aligned} A_{0,m_z} &= -\frac{\Phi_{0,m_z}}{\int_0^1 dz \psi_c \cdot \overline{\psi_c^*}} \int_0^1 dz (w_c D \psi_{0,m_z} + (i\alpha_x u_{0,m_z} + i\alpha_y v_{0,m_z}) \psi_c) \cdot \overline{\psi_c^*}, \\ A_{2,m_z} &= -\frac{\Phi_{2c,m_z}}{\int_0^1 dz \psi_c \cdot \overline{\psi_c^*}} \int_0^1 \left( 2D\overline{w_c} \psi_{2c,m_z} + \overline{w_c} D \psi_{2c,m_z} + \frac{1}{2} Dw_{2c,m_z} \overline{\psi_c} + w_{2c,m_z} D \overline{\psi_c} \right) \cdot \overline{\psi_c^*}, \\ \Phi_{0,m_z} &= \frac{1}{\beta_{0,m_z} \int_0^1 dz \psi_{0,m_z} \cdot \overline{\psi_{0,m_z}^*}} \int_0^1 dz 2 \operatorname{Re} \{ (Dw_c + w_c D) \overline{\psi_c} \} \cdot \overline{\psi_{0,m_z}^{*k}}, \\ \Phi_{2c,m_z} &= \frac{-1}{(2i \operatorname{Im}(\beta_c) - \beta_{2c,m_z}) \int_0^1 dz \psi_{2c,m_z} \cdot \overline{\psi_{2c,m_z}^*}} \int_0^1 (-Dw_c + w_c D) \psi_c \cdot \overline{\psi_{2,m_z}^*}. \end{aligned}$$

The numerical strategy is as follows. Initially we fix all parameters and compute the eigenvalues for the first few wave indices  $(m_x^c, m_y^c)$  numerically, and call the minimum of these eigenvalue  $\beta_c$ . Next we vary one of the parameters, say  $\Lambda$ , to determine the critical value of  $\Lambda_c$ , so that  $\operatorname{Re} \beta_c(\Lambda_c) = 0$ . Then we fix  $\Lambda = \Lambda_c$  and find all the eigenpairs corresponding to wave indices  $(0, 0)$  and  $2(m_x^c, m_y^c)$  and compute the transition number using (8.3).

## 9. NUMERICAL INVESTIGATIONS

**9.1. Parameters vs Critical Eigenvalue.** According to (5.1), increasing the parameters  $\operatorname{Fr}$ ,  $\operatorname{Ro}$ ,  $\operatorname{Pr}$  has a stabilizing effect while increasing  $\Lambda$  has a destabilizing effect on the eigenvalue  $\beta_c$  with largest real part. We verify this numerically in Figure 9.1 where the first real part of the eigenvalue is plotted against the system parameters for fixed wave number  $\alpha$ . The first and last plots of Figure 9.1 also show that the eigenvalue of largest real part is always bounded below by  $\operatorname{Re} \beta_{001}^k$  ( $k = 1, 2, 3$ ).

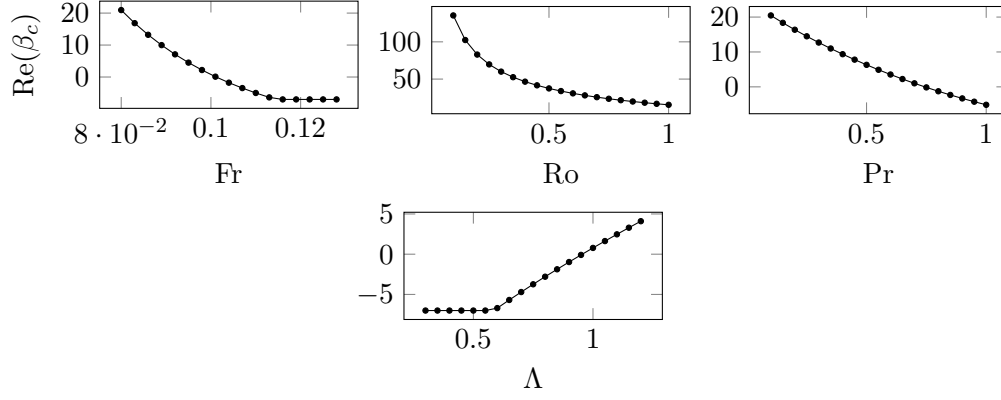


FIGURE 9.1. The real part of the first eigenvalue when the system parameters are fixed  $L_x = 2$ ,  $L_y = 2$ ,  $\text{Fr} = 0.1$ ,  $\Lambda = 1$ ,  $\text{Pr} = 0.71$ ,  $\text{Ro} = 2$  except for one of them which is varied.

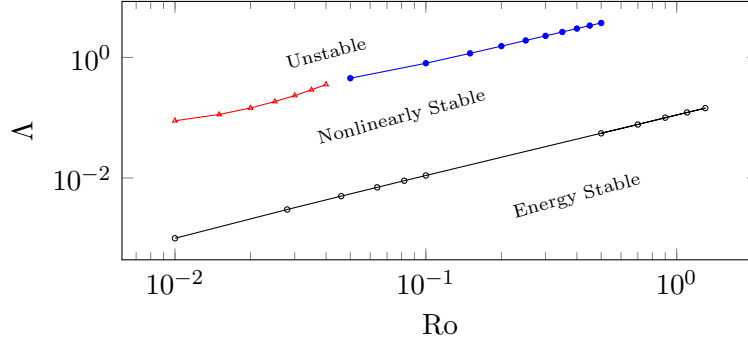


FIGURE 9.2. Stability curves for  $\text{Pr} = 0.71$ ,  $\text{Fr} = 0.2$ ,  $L_x = L_y = 1.0$ . The curve indicates transition to multiple equilibria ( $\blacktriangle$ ), transition to spatio-temporal oscillations ( $\bullet$ ) and energy stability ( $\circ$ ).

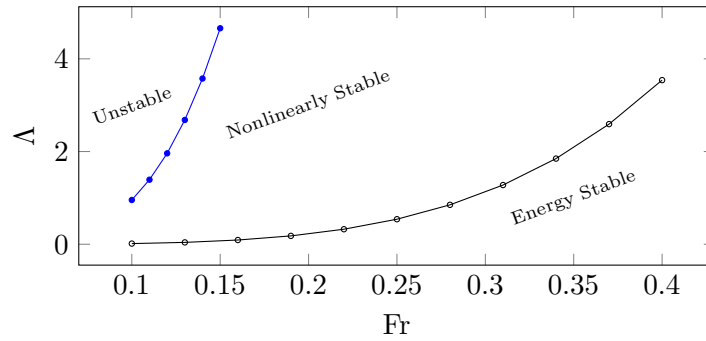


FIGURE 9.3. Stability curves for  $\text{Pr} = 0.71$ ,  $\text{Ro} = 2$ ,  $L_x = 1$  and  $L_y = 1$ . The curve indicates transition to multiple equilibria ( $\bullet$ ) and energy stability ( $\circ$ ).

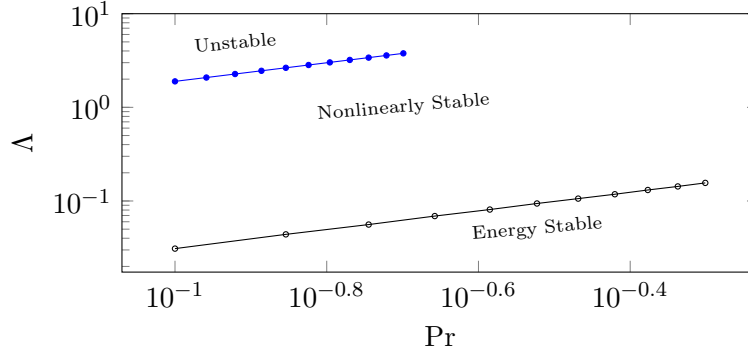


FIGURE 9.4. Stability curves for  $Fr = 0.2$ ,  $Ro = 2$ ,  $L_x = L_y = 1$ . The curve indicates transition to multiple equilibria ( $\bullet$ ) and energy stability ( $\circ$ ).

**9.2. Stability Diagrams.** Figures 9.2 and Figure 9.3 show several stability regions in the parameter space. In both figures, a cubic basin  $L_x = 1$ ,  $L_y = 1$  is chosen and the Prandtl number is fixed at  $Pr = 0.71$ .

Figure 9.2 investigates the stability of the system in the  $Ro-\Delta$  plane. The figure shows that the system has energy stability for small  $\Delta$ . As  $\Delta$  increases, the system becomes nonlinearly stable and finally a dynamic transition occurs, either to spatiotemporal oscillations or to multiple equilibria depending on  $Ro$ , as indicated in Theorem 6.1. The curves leading to different transitions seem to intersect at a single point, where the reduced system will become four dimensional.

Figure 9.3 investigates the stability of the system in the  $Fr-\Delta$  plane. The figure shows that once again the system has energy stability for small  $\Delta$ . As  $\Delta$  increases, the system becomes nonlinearly stable and finally a dynamic transition occurs. In this case we find that the system exhibits only transitions to multiple equilibria depending on  $Ro$ .

**9.3. The Transition Number.** We demonstrate some numerical details, namely the coefficients of the center manifold function and the nonlinear interactions contributing to the transition number in Table 1. For the given parameters in Table 1, the critical value  $\Delta_c$  and the critical wave indices  $(m_x^c, m_y^c)$  are found. The critical eigenvalues are real, and the transition number is negative. According to the main dynamic theorem, Theorem 6.1, the system bifurcates from the basic shear flow to a stable circle of steady states. In Table 1, we note that some of the coefficients of the center manifold is zero due to the even-odd symmetries of the eigenvectors, canceling some of the integrations.

In Figure 9.5, the values of transition number  $A$  is shown in a parameter regime. In the case of very low  $Ro$  numbers it is seen from the first plot that the transition is to spatiotemporal oscillations. Also observed in this case is that the real part of the transition number admits both negative and positive values indicating both continuous and catastrophic transitions. As the  $Ro$  number increases, the transition becomes a continuous one to multiple steady states. In the second plot of Figure 9.5 we test the transition number against the Froude number and find that the transition is continuous and is to multiple steady states.

TABLE 1. Real and imaginary parts of the numerical values for the center manifold and transition number evaluated for the parameter values  $L_x = 1$ ,  $L_y = 1$ ,  $\text{Fr} = 0.2$ ,  $\text{Pr} = 0.71$ ,  $\text{Ro} = .1$ ,  $\Lambda = \Lambda_c = 0.799$  and  $(m_x^c, m_y^c) = (0, 1)$ . The transition number is  $A = \sum_{m_z=1}^6 A_{0,m_z} + A_{2,m_z} = -0.0147 + 0.0021 = -0.0126$ .

$m_z$	$\text{Re } \Phi_{0,m_z}$	$\text{Im } \Phi_{0,m_z}$	$\text{Re } \Phi_{2,m_z}$	$\text{Im } \Phi_{2,m_z}$	$\text{Re } A_{0,m_z}$	$\text{Im } A_{0,m_z}$	$\text{Re } A_{2,m_z}$	$\text{Im } A_{2,m_z}$
1	$-1 \cdot 10^{-17}$	$1 \cdot 10^{-17}$	$-3 \cdot 10^{-2}$	$1 \cdot 10^{-3}$	$8 \cdot 10^{-19}$	$-4 \cdot 10^{-18}$	$2 \cdot 10^{-3}$	$7 \cdot 10^{-17}$
2	$-1 \cdot 10^{-17}$	$-1 \cdot 10^{-17}$	$-6 \cdot 10^{-4}$	$1 \cdot 10^{-4}$	$-8 \cdot 10^{-19}$	$-4 \cdot 10^{-18}$	$5 \cdot 10^{-5}$	$2 \cdot 10^{-19}$
3	$4 \cdot 10^{-17}$	0	$1 \cdot 10^{-5}$	$-4 \cdot 10^{-6}$	$-5 \cdot 10^{-33}$	$-2 \cdot 10^{-18}$	$-6 \cdot 10^{-7}$	$2 \cdot 10^{-18}$
4	$-2 \cdot 10^{-2}$	$1 \cdot 10^{-3}$	$-5 \cdot 10^{-3}$	$-3 \cdot 10^{-3}$	$-1 \cdot 10^{-2}$	$-1 \cdot 10^{-3}$	$-2 \cdot 10^{-4}$	$-2 \cdot 10^{-4}$
5	$-2 \cdot 10^{-2}$	$-1 \cdot 10^{-3}$	$5 \cdot 10^{-3}$	$2 \cdot 10^{-3}$	$-1 \cdot 10^{-2}$	$1 \cdot 10^{-3}$	$-2 \cdot 10^{-4}$	$2 \cdot 10^{-4}$
6	$1 \cdot 10^{-2}$	0	$-1 \cdot 10^{-4}$	$5 \cdot 10^{-4}$	$9 \cdot 10^{-3}$	$-4 \cdot 10^{-18}$	$-1 \cdot 10^{-5}$	$3 \cdot 10^{-18}$

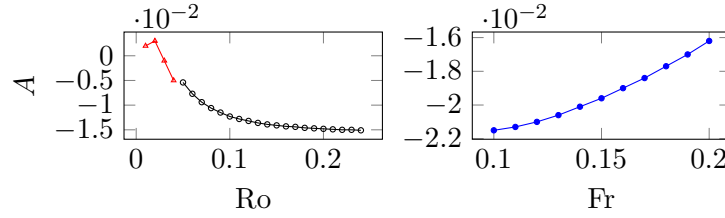


FIGURE 9.5. The transition number  $A$  at fixed  $L_x = 1$ ,  $L_y = 1$ ,  $\text{Fr} = 0.2$ ,  $\Lambda = \Lambda_c$ ,  $\text{Pr} = 0.71$ ,  $\text{Ro} = 2$  except for the one which is varied. The curve ( $\text{---}\bullet\text{---}$ ) shows the real part of the transition number where the transition is to spatio-temporal oscillations. In ( $\text{---}\bullet\text{---}$ ) and ( $\text{---}\bullet\text{---}$ ), the transition is to multiple steady states.

**9.4. Critical Eigenvectors.** Figure 9.6 displays the real and imaginary parts of the  $z$ -dependence of the density and velocity profiles of the first critical eigenvector for the given parameter values. The wave index of this critical mode is found to be  $(m_x^c, m_y^c) = (0, 1)$ . This is a roll pattern parallel to the  $x$ -axis. The skewed roll structure of the first critical eigenmodes can be seen in Figure 9.7.

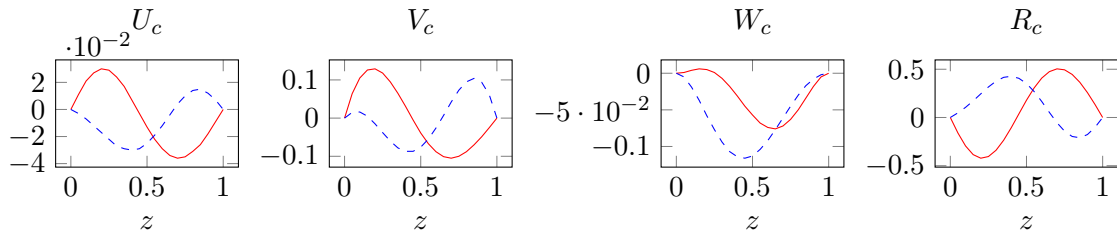


FIGURE 9.6. The real part ( $\text{---}$ ) and the imaginary part ( $\text{---}$ ) of the  $z$  dependence of the density and the velocity profiles of the first critical eigenvector at  $L_x = L_y = 1$ ,  $\text{Fr} = 0.2$ ,  $\text{Pr} = 0.71$ ,  $\text{Ro} = 0.1$ ,  $\Lambda = \Lambda_c$ . Here  $(m_x^c, m_y^c) = (0, 1)$ .

**9.5. Critical Wave Number Selection and Pattern Formation.** In this section, we give some remarks on the selection of the critical wave number and its implications on the pattern formation.

We fix the parameters as  $\text{Fr} = 0.2$ ,  $\text{Pr} = 0.71$  and  $\text{Ro} = 0.1$  and obtain the Figure 9.8 describing the selection of wave indices for the critical eigenmodes.



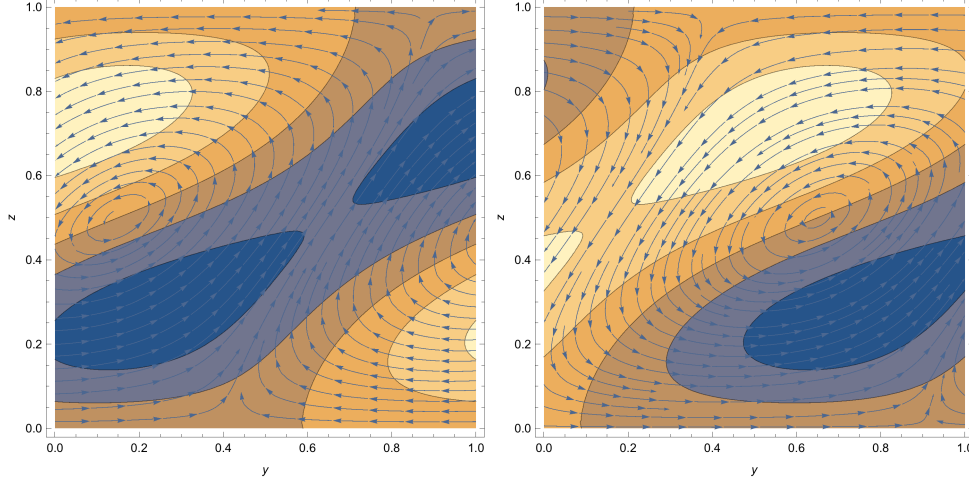


FIGURE 9.7. The real and imaginary parts of  $(v_c, w_c)$ -vector field on top of the contour plot of the critical density field in the  $yz$ -plane for  $L_x = L_y = 1$ ,  $Fr = 0.2$ ,  $Pr = 0.71$ ,  $Ro = 0.1$ ,  $\Lambda = \Lambda_c$ . Here  $(m_x^c, m_y^c) = (0, 1)$ .

From Figure 9.8 at the indicated parameters, we observe that regardless of the horizontal length scale  $L_x$ , the wave indices are given by  $(0, 1)$  if  $L_y < 1.74$ ,  $(0, 2)$  if  $1.74 < L_y < 2.96$ ,  $(0, 3)$  if  $2.96 < L_y < 4.17$ . We observed the similar behavior for the selection of the critical wave indices in our other numerical experiments.

Thus the first critical modes always consist of  $m_y$ -rolls aligned with the  $x$ -axis irrespective of  $L_x$ . Moreover  $m_y$ , the number of rolls increases as  $L_y$  is increased.

It is interesting that the system does not seem to admit rectangle modes (i.e.  $(m_x, m_y)$  with  $m_x \neq 0$  and  $m_y \neq 0$ ) or rolls parallel to the  $y$ -axis.

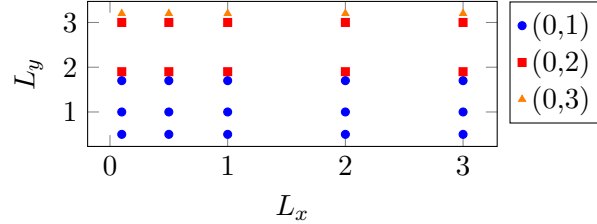


FIGURE 9.8. The selection of the critical wave number at  $Fr = 0.2$ ,  $Pr = 0.71$  and  $Ro = 0.1$ .

## 10. CONCLUSIONS

We find a criterion for the energy stability of the system in terms of system parameters.

By studying the linear stability of the problem, we find a criterion for the nonlinear stability of the system. Our numerical investigations show the existence of a hypersurface  $\Lambda = \Lambda_c$  which separates the parameter space into regions where the basic shear flow is stable and unstable. More explicit expression for  $\Lambda_c$  is not given in this article, and will be addressed in a later study.

Numerical investigations also yield that selection of horizontal wave indices at fixed  $Fr$ ,  $Pr$ ,  $Ro$  is determined by only  $L_y$  and is independent of  $L_x$ . We find that the system admits only critical eigenmodes with horizontal wave indices  $(0, m_y)$ . Such modes, horizontally have the pattern consisting of  $m_y$ -rolls aligned with the  $x$ -axis.

We show under the assumption of critical crossing of eigenvalues that the system exhibits dynamic transitions to both multiple steady states and spatiotemporal oscillations. In both cases, the

transition can be either continuous, represented by local attractors close to the basic shear flow, or catastrophic, represented by local attractors far away from the basic shear flow. Numerically we encountered continuous transitions to multiple steady states, continuous and catastrophic transitions to spatiotemporal oscillations.

Another contribution of this paper is the derivation of a representation of the center manifold approximation in the case of a pair of complex conjugate eigenvalues, adapting similar results [16] to the present case. This new representation allows to write a unified transition number covering both the double real eigenvalue and a pair of complex conjugate eigenvalue cases.

## APPENDIX A. APPROXIMATION OF CENTRAL MANIFOLD FUNCTIONS

In this section we derive a new representation for the approximation of the center manifold function suitable for studying problems in spatial domains with periodicity condition in at least one direction. General approximate formulas for center manifold functions were first introduced [14, 13, 16], and have played central role in a wide range of applications of the dynamic transition theory.

We follow the same framework as in [16]. Let  $X$  and  $X_1$  be two Banach spaces and  $X_1 \subset X$  a compact and dense inclusion. Consider the following evolution equation

$$(A.1) \quad \begin{aligned} \frac{d\phi}{dt} &= L_\lambda \phi + G(\phi, \lambda), \\ \phi(0) &= \varphi, \end{aligned}$$

where  $\phi$  is the unknown function and  $\lambda \in \mathbb{R}$  is the parameter.

We assume that  $L_\lambda = -A + B_\lambda : X_1 \rightarrow X$  is a linear completely continuous field, where  $A : X_1 \rightarrow X$  is a linear homeomorphism and  $B_\lambda : X_1 \rightarrow X$  is a linear compact operator. Furthermore we assume that  $L_\lambda$  is a sectorial operator depending continuously on  $\lambda$ . In this case, we can define the fractional order spaces  $X_\alpha = D(L_\lambda^\alpha)$  for  $\alpha \in \mathbb{R}$ . We also assume that  $G(\cdot, \lambda) : X_\theta \rightarrow X$  is  $C^r$  ( $r \geq 1$ ) bounded mapping for some  $0 \leq \theta < 1$ , depending continuously on  $\lambda \in \mathbb{R}$  and

$$(A.2) \quad G(\phi, \lambda) = o(\|\phi\|_{X_\theta}) \quad \forall \lambda \in \mathbb{R}.$$

We know that for a linear completely continuous field, the spectrum consists of isolated eigenvalues with finite dimensional eigenspaces. Let  $\{\beta_i(\lambda) \in \mathbb{C} \mid i \in \mathbb{N}\}$  be all eigenvalues of  $L_\lambda$  counting multiplicities and  $\{\phi_i(\lambda) \mid i \in \mathbb{N}\}$  be the corresponding (complex) eigenvectors. Assume that the following principle of exchange of stabilities (PES) condition holds true:

$$(A.3) \quad \begin{aligned} \operatorname{Re} \beta_1 = \operatorname{Re} \beta_2 &\begin{cases} < 0 & \text{if } \lambda < \lambda_0, \\ = 0 & \text{if } \lambda = \lambda_0, \\ > 0 & \text{if } \lambda > \lambda_0, \end{cases} \\ \operatorname{Re} \beta_j(\lambda_0) &< 0 \quad \text{for } j \geq 3. \end{aligned}$$

Assume the eigenpairs satisfy

$$\beta_1 = \overline{\beta_2}, \quad \phi_1 = \overline{\phi_2}.$$

By the spectral theorem [14, 16], the spaces  $X_1$  and  $X$  can be decomposed into the direct sum

$$X_1 = E_1^\lambda \oplus E_2^\lambda, \quad X = E_1^\lambda \oplus \overline{E_2^\lambda},$$

where

$$\begin{aligned} E_1^\lambda &= \operatorname{span}\{z\phi_1(\lambda) + \overline{z\phi_1(\lambda)} \mid z \in \mathbb{C}\}, \\ E_2^\lambda &= \text{the complement of } E_1^\lambda \text{ in } X. \end{aligned}$$

Then  $L_\lambda$  is invariant on  $E_1^\lambda$  and  $E_2^\lambda$ , i.e.,  $L_\lambda$  can be decomposed as

$$(A.4) \quad \begin{aligned} L_\lambda &= \mathcal{J}_\lambda \oplus \mathcal{L}_\lambda, \\ \mathcal{J}_\lambda &: E_1^\lambda \rightarrow E_1^\lambda, \\ \mathcal{L}_\lambda &: X_1 \cap E_2^\lambda \rightarrow E_2^\lambda. \end{aligned}$$

Finally let  $P_i$  be the projection onto  $E_i^\lambda$ . Below we omit  $\lambda$ 's to simplify the notation.

**Lemma A.1.** *Assume  $G$  defined in (A.1) is a bilinear operator. Let*

$$x(t) = z(t)\phi_1 + \overline{z(t)\phi_1} \in E_1.$$

*Under the above assumptions, for  $\lambda$  sufficiently close to  $\lambda_0$  we have the following approximation for the center manifold function*

$$(A.5) \quad \Phi(x(t), \lambda) = (2i \operatorname{Im}(\beta_1) - \mathcal{L})^{-1} P_2 G(z\phi_1, z\phi_1) + (-\mathcal{L})^{-1} P_2 G(z\phi_1, \overline{z\phi_1}) + o(2) + \text{c.c.},$$

*where c.c. stands for the complex conjugate of the whole expression coming before and  $o(k)$  stands for*

$$(A.6) \quad o(k) := o(\|x\|_{X_1}^k) + O(|\operatorname{Re} \beta_1(\lambda)| \|x\|_{X_1}^k).$$

*Proof.* It is known that the center manifold can be approximated by

$$(A.7) \quad \Phi = \int_{-\infty}^0 e^{-\tau \mathcal{L}} \rho_\epsilon P_2 G(e^{\tau \mathcal{J}} x) d\tau + o(k),$$

where  $\mathcal{J} = \operatorname{diag}(\beta_1, \overline{\beta_1})$  so that  $e^{\tau \mathcal{J}} x = e^{\tau \beta_1} z\phi_1 + \overline{e^{\tau \beta_1} z\phi_1}$  with  $\rho_\epsilon$  denoting a cut-off function. Hence

$$G(e^{\tau \mathcal{J}} x) = e^{2\tau \beta_1} G(z\phi_1, z\phi_1) + e^{\tau(\beta_1 + \overline{\beta_1})} G(z\phi_1, \overline{z\phi_1}) + \text{c.c.}$$

Let  $P_2 G(z\phi_1, z\phi_1) = \sum_{m \geq 3} g_m \phi_m$  and  $P_2 G(z\phi_1, \overline{z\phi_1}) = \sum_{m \geq 3} h_m \phi_m$ . Then

$$(A.8) \quad \begin{aligned} \Phi &= \int_{-\infty}^0 e^{-\tau \mathcal{L}} \sum_{m \geq 3} (e^{2\tau \beta_1} g_m + e^{\tau(\beta_1 + \overline{\beta_1})} h_m) \phi_m d\tau + \text{c.c.} + o(2) \\ &= \sum_{m \geq 3} \int_{-\infty}^0 (e^{-\tau(\beta_m - 2\beta_1)} g_m + e^{-\tau(\beta_m - \beta_1 - \overline{\beta_1})} h_m) \phi_m d\tau + \text{c.c.} + o(2). \end{aligned}$$

The following integrals converge by the PES condition, since  $\operatorname{Re}(\beta_m - 2\beta_1) < 0$ :

$$\begin{aligned} \int_{-\infty}^0 e^{-\tau(\beta_m - 2\beta_1)} d\tau &= \frac{1}{2\beta_1 - \beta_m} = \frac{1}{2i \operatorname{Im}(\beta_1) - \beta_m} + O(|\operatorname{Re} \beta_1|), \\ \int_{-\infty}^0 e^{-\tau(\beta_m - \beta_1 - \overline{\beta_1})} d\tau &= \frac{1}{2 \operatorname{Re}(\beta_1) - \beta_m} = -\frac{1}{\beta_m} + O(|\operatorname{Re} \beta_1|). \end{aligned}$$

Plugging these expressions in (A.8), we obtain

$$\Phi = \sum_{m \geq 3} \left( \frac{1}{2i \operatorname{Im}(\beta_1) - \beta_m} g_m - \frac{1}{\beta_m} h_m \right) \phi_m + \text{c.c.} + o(2),$$

from which the result follows.  $\square$

**Remark.** *We note that the approximation in (A.5) is valid whether  $\operatorname{Im} \beta_c \neq 0$  or not. In the case  $\operatorname{Im} \beta_c = 0$ , it is very easily seen that the formula reduces to the case*

$$(A.9) \quad \Phi(x(t), \lambda) = -\mathcal{L}^{-1} P_2 G(x(t)) + o(2),$$

*which was first derived in [14, 13].*

## REFERENCES

- [1] V. BJERKNES, *Das Problem der Wettervorhersage: betrachtet vom Standpunkte der Mechanik und der Physik*, 1904.
- [2] M. CAI, *An analytic study of the baroclinic adjustment in a quasigeostrophic two-layer channel model*, Journal of the atmospheric sciences, 49 (1992), pp. 1594–1605.
- [3] M. CAI AND M. MAK, *On the multiplicity of equilibria of baroclinic waves*, Tellus A, 39 (1987), pp. 116–137.
- [4] J. CHARNEY, *On the scale of atmospheric motion*, Geofys. Publ., 17(2) (1948), pp. 1–17.
- [5] H. DIJKSTRA, T. SENGÜL, J. SHEN, AND S. WANG, *Dynamic Transitions of Quasi-geostrophic Channel Flow*, SIAM Journal on Applied Mathematics, 75 (2015), pp. 2361–2378.
- [6] H. A. DIJKSTRA, *Nonlinear Physical Oceanography: A Dynamical Systems Approach to the Large Scale Ocean Circulation and El Niño.*, Kluwer Academic Publishers, Dordrecht, the Netherlands, 2000.
- [7] H. A. DIJKSTRA AND M. GHIL, *Low-frequency variability of the large-scale ocean circulations: a dynamical systems approach*, Review of Geophysics, 43 (2005), pp. 1–38.
- [8] E. T. EADY, *Long waves and cyclone waves*, Tellus, 1 (1949), pp. 33–52.
- [9] M. GHIL AND S. CHILDRESS, *Topics in Geophysical Fluid Dynamics: Atmospheric Dynamics, Dynamo Theory, and Climate Dynamics*, Springer-Verlag, New York, 1987.
- [10] J.-L. LIONS, R. TEMAM, AND S. WANG, *New formulations of the primitive equations of atmosphere and applications*, Nonlinearity, 5 (1992), pp. 237–288.
- [11] E. N. LORENZ, *Deterministic nonperiodic flow*, J. Atmos. Sci., 20 (1963), pp. 130–141.
- [12] ———, *The mechanics of vacillation*, J. Atmos. Sci., 20 (1963), pp. 448–464.
- [13] T. MA AND S. WANG, *Bifurcation and stability of superconductivity*, J. Math. Phys., 46 (2005), pp. 095112, 31.
- [14] ———, *Bifurcation theory and applications*, vol. 53 of World Scientific Series on Nonlinear Science. Series A: Monographs and Treatises, World Scientific Publishing Co. Pte. Ltd., Hackensack, NJ, 2005.
- [15] ———, *Dynamic transition theory for thermohaline circulation*, Phys. D, 239 (2010), pp. 167–189.
- [16] ———, *Phase Transition Dynamics*, Springer-Verlag, 2013.
- [17] M. MAK, *Equilibration in nonlinear baroclinic instability*, Journal of the atmospheric sciences, 42 (1985), pp. 2764–2782.
- [18] J. PEDLOSKY, *Finite-amplitude baroclinic waves*, Journal of the Atmospheric Sciences, 27 (1970), pp. 15–30.
- [19] N. A. PHILLIPS, *The general circulation of the atmosphere: A numerical experiment*, Quart J Roy Meteorol Soc, 82 (1956), pp. 123–164.
- [20] C. ROSSBY, *On the solution of problems of atmospheric motion by means of model experiment*, Monthly Weather Review, 54 (1926), pp. 237–240.
- [21] H. STOMMEL, *Thermohaline convection with two stable regimes of flow*, Tellus, 13 (1961), pp. 224–230.
- [22] G. VERONIS, *An analysis of wind-driven ocean circulation with a limited fourier components*, J. Atmos. Sci., 20 (1963), pp. 577–593.
- [23] ———, *Wind-driven ocean circulation, part ii: Numerical solution of the nonlinear problem*, Deep-Sea Res., 13 (1966), pp. 31–55.
- [24] J. VON NEUMANN, *Some remarks on the problem of forecasting climatic fluctuations*, in Dynamics of climate, R. L. Pfeffer, ed., Pergamon Press, 1960, pp. 9–12.
- [25] S. ÖZER AND T. ŞENGÜL, *Stability and transitions of the second grade poiseuille flow*, Physica D: Nonlinear Phenomena, 331 (2016), pp. 71 – 80.

(Şengül) DEPARTMENT OF MATHEMATICS, MARMARA UNIVERSITY, 34722 ISTANBUL, TURKEY  
*E-mail address:* `taylan.sengul@marmara.edu.tr`

(Wang) DEPARTMENT OF MATHEMATICS, INDIANA UNIVERSITY, BLOOMINGTON, IN 47405  
*E-mail address:* `showang@indiana.edu`, <http://www.indiana.edu/~fluid>